Structural Ordering on Physical Gelation of Syndiotactic Polystyrene Dispersed in Chloroform Studied by Time-Resolved Measurements of Small Angle Neutron Scattering (SANS) and Infrared Spectroscopy

Masamichi Kobayashi* and Toshinori Yoshioka

Department of Macromolecular Science, Faculty of Science, Osaka University, Toyonaka, Osaka 560, Japan

Masayuki Imai and Yuji Itoh

Neutron Scattering Laboratory, Institute of Solid State Physics, University of Tokyo, Tokai-mura, Ibaraki 319-11, Japan

Received February 10, 1995; Revised Manuscript Received July 25, 1995®

ABSTRACT: Physical gelation of syndiotactic polystyrene (SPS) dispersed in chloroform was found to proceed very slowly in the time scale of 10 h or longer. Time evolution of gel-network structure on the gelation process was investigated by time-resolved measurements of small angle neutron scattering (SANS) and Fourier transform infrared (FT-IR) spectroscopy for various combinations of such factors as the molecular weight of SPS (M_w), the polymer concentration (C), and temperature, on which the kinetic behavior of the gelation depends remarkably. For every case, the total SANS intensity Q, as a measure of the degree of gelation, increased with time in parallel to the TTGG-type conformational ordering of the SPS molecules dispersed in the gel measured by time-resolved FT-IR. At an early stage of gelation, the SANS functions were reproduced well by the equation presented by Dozier et al. for semidilute solutions of star polymers and then converted to the form characteristic of continuous fractal objects as the gelation proceeded. The parameters describing gel-network structure, such as the radius of gyration of stars R_g, the correlation length ξ', and the mass-fractal dimension D' inside the star were evaluated as a function of gelation time through a nonlinear least squares fitting. ξ' and D' were found to exhibit a divergence-like abrupt change at a particular gelation time. At the same time the Q and the conformational order started to increase, indicating that the sol−gel transformation occurred at this point. The sol−gel transformation was found to be delayed with lowering M_w or C or with raising temperature. The time dependencies of the SANS functions after the transformation regime was analyzed by the theoretical equation derived by Freltoft et al. for continuous fractal objects.

Introduction

Syndiotactic polystyrene (abbreviated as SPS) is a typical synthetic stereoregular polymer situated at the counterpart of isotactic polystyrene (IPS). In crystalline phases, SPS molecules assume two types of ordered skeletal conformations although various crystal modifications have been found so far; one is the TT (*trans−trans*) type which constructs a planar zigzag chain, and the other is the TTGG (*trans−trans−gauche−gauche*) type constructing a (2/1) helical chain (Figure 1).[1−8]

This polymer is soluble in various organic solvents at elevated temperatures, and the hot solutions convert to transparent gels by allowing them to stand at room temperature. Infrared spectra of the gels thus prepared indicate that highly ordered sequences of the TTGG-type skeletal conformation are formed on gelation.[9,10] The type of the ordered conformation is the same regardless of the solvent in which the SPS molecules are dispersed, but the rates of gelation as well as of the accompanied conformational ordering are strongly dependent on the solvent. For example, in the cases of SPS/carbon tetrachloride (CCl_4) and SPS/o-dichlorobenzene (o-$C_6H_4Cl_2$) systems the gelation is accomplished within a few minutes at room temperature, while in the SPS/chloroform ($CHCl_3$) system it proceeds very slowly with the time scale of several tens of hours or longer. The kinetic behaviors of the conformational ordering in the SPS/chloroform system were investigated by means of time-resolved Fourier transform infrared (FT-IR) spectroscopy, and it was revealed that the ordered TTGG sequences were formed and stabilized by clustering of a certain number of polymer segments.[11] The number of the clustering segments was estimated experimentally as five around 10 °C and decreased with lowering temperature, approaching unity below −10 °C (for the case of $M_w = 36 \times 10^4$), indicating that the ordering mechanism crosses over from the chain clus-

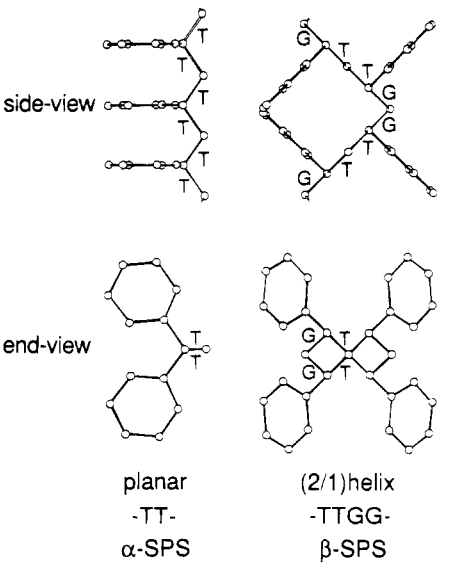

Figure 1. Two ordered skeletal conformations, TT and TTGG, of syndiotactic polystyrene in the crystalline phase.

® Abstract published in *Advance ACS Abstracts,* September 15, 1995.

0024-9297/95/2228-7376$09.00/0

tering to the self-organization within one chain.[11]

The physical gelation is basically a macroscopic phenomenon accompanied with immobilization of the system as a whole caused by formation of networks via aggregation of polymer molecules. Therefore, elucidation of the molecular aggregation process is indispensable for understanding the mechanism of gelation. For studying the state of polymer aggregates with sizes of several tens of nanometers, the small angle neutron scattering (SANS) technique is powerful. Since gelation of the SPS/$CHCl_3$ system proceeds very slowly, we are able to investigate the time evolution of polymer aggregation on the gelation process by means of time-resolved measurements of SANS.

In the present work, the SANS profiles of SPS/$CHCl_3$ gels obtained as a function of gelation time were analyzed quantitatively and the time dependencies of some structural parameters describing the aggregation states of polymer molecules were derived for various sets of molecular weight, concentration, and temperature. The results obtained were compared with those of the molecular-level conformational ordering studied by time-resolved FT-IR spectroscopy.

Experimental Section

Samples. The SPS samples with weight average molecular weights (M_w) of 113.5 × 10^4, 36 × 10^4, and 23.1 × 10^4 (measured by GPC) supplied from Idemitsu Kosan Co. Ltd. were used without further fractionation. The samples used for time-resolved SANS experiments were prepared by the following process. The polymer was dissolved in deuterated chloroform ($CDCl_3$) in a sealed glass ampule at about 100 °C (above the boiling point of $CDCl_3$, 61.2 °C at atmospheric pressure). The polymer concentration C was determined from the amounts of the polymer and solvent weighed into the ampule.

As the sample cells for the SANS experiments, pairs of sealed-type quartz cells with various optical path lengths were used depending on C. The polymer solution prepared in a sealed ampule was transferred into the quartz cell by using a syringe warmed to prevent the hot solution from gelation during the transfer. The filled quartz cell was sealed with a Teflon stopper and heated again until the interior was dissolved. After the sample thus prepared was set on a cell stand in the sample chamber kept at a preset desired temperature, a series of time-resolved SANS measurements started at the time interval of 30 min. For the measurements of time-resolved FT-IR, the hot solution prepared in a sealed ampule was transferred into a homemade optical cell with KBr windows whose optical path length was adjusted to a suitable value depending on C by changing the thickness of the lead spacer inserted between the windows. The filled cell was set on the holder kept at a preset temperature and subjected to a series of time-resolved measurements at a suitable time interval.

SANS Measurements. The SANS experiments were carried out in the Neutron Scattering Laboratory of the Institute for Solid State Physics, University of Tokyo, using the SANS-U instrument situated at the end of a cold-neutron guide tube from the JRR-3 reactor of the Japan Atomic Energy Research Institute. For the present work, neutron wavelength $\lambda = 0.70$ nm was used. The distance (L) from the sample to the two-dimensional position-sensitive detector (PSD) was set at 4.0 m. The data taken cover the momentum transfer q range of 0.08−1.00 nm^{-1} [$q = (4\pi/\lambda)\sin(\theta/2)$; θ is the scattering angle]. For every pair of gel and solvent, the scattering intensities as a function of q and the transmissions for the neutron beam, T_{gel} and T_{solv}, were measured. After background and normalization corrections, the intensity data recorded on the PSD were radially averaged, resulting in scattering functions of $I(q)_{gel}$ and $I(q)_{solv}$. The scattering function for the solvent and the contribution of the incoherent scattering I_{inc} were subtracted from that of the gel

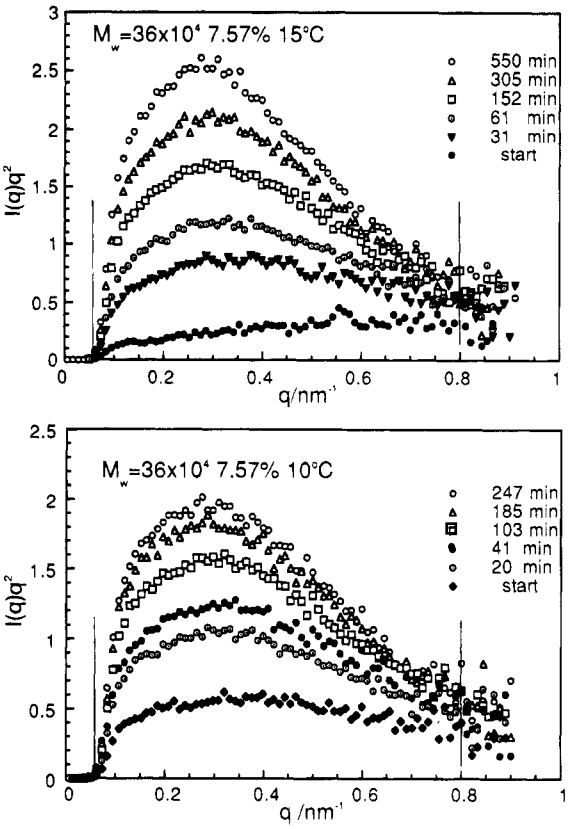

Figure 2. Time dependency of the SANS function represented by the Kratky plot on gelation measured for SPS (M_w = 36 × 10^4, C = 7.57 g/dL)/$CDCl_3$ at 15 and 10 °C. The vertical lines denote the area of integration for calculating the invariant Q.

$$I(q) = I(q)_{gel} - I(q)_{solv}\left(\frac{T_{gel}}{T_{solv}}\right) - I_{inc} \quad (1)$$

giving the corrected scattering function $I(q)$ due to the polymeric materials embedded in a solvent matrix. The correction for the background due to the I_{inc} arising from hydrogenated SPS molecules was performed by the following procedure. The scattering intensities of $I(q)_{gel} - I(q)_{solv}(T_{gel}/T_{solv})$ at the tail in the high q range (q = 1.5−1.8 nm^{-1}) were measured with the PSD placed at L = 1.5 m, the ratio of the scale factors between the intensities measured with the PSD set at L = 4 and 1.5 m being evaluated by using a standard Lupolene sample. The tail intensities (per unit polymer concentration C and unit optical path length) were found to decrease more or less with a decrease in C. This trend is presumably due to a C-dependent contribution of the coherent scattering contained in the intensity at the tail. The intensity extrapolated to C = 0 was regarded as I_{inc} per unit concentration and unit optical path length.

FT-IR Measurement. Time-resolved FT-IR measurements were performed at various concentrations and temperatures using a JASCO FT-IR 8300 spectrometer equipped with a DTGS detector. The spectral resolution was set at 1 cm^{-1}. For the measurements at low temperatures, the sample cell was set on the cold finger of an Oxford flow-type cryostat and the temperature was controlled within ±1 °C.

Results and Discussion

1. Time Evolution of Gel-Network Formation on Gelation. An example of time dependencies of the $I(q)$ functions obtained is shown in Figure 2 by the Kratky plot [the $I(q)q^2$ vs q plot] for the cases of C = 7.57 g/dL at 15 and 10 °C. We mention here the time evolution of the total amount of polymeric aggregates formed in gels. The scattering intensity around q = 0.3 nm^{-1} gets stronger with gelation time. The amount of the poly-

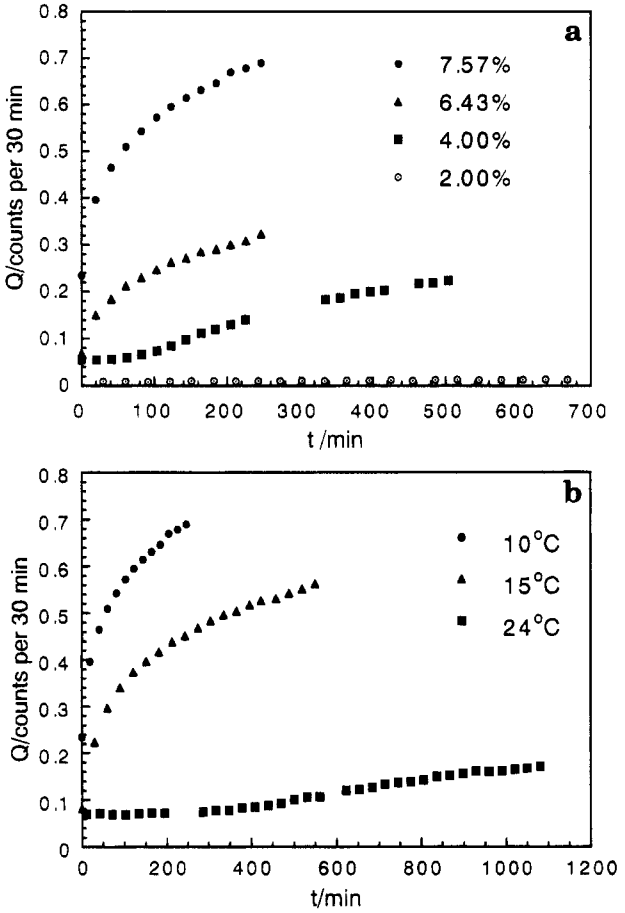

Figure 3. Time evolution of total SANS intensity Q on gelation measured for SPS (M_w = 36 × 10⁴)/$CDCl_3$: (a) concentration dependence measure at 10 °C; (b) temperature dependence measured at C = 7.57 g/dL.

meric aggregates is proportional to the total scattering intensity or the invariant Q defined as

$$Q = 4\pi \int I(q)\, q^2\, dq \qquad (2)$$

Here, the integration was made in the limited range of q = 0.06−0.8 nm^{-1}; then the values obtained are of the "partial invariant" which is considered to be a measure of the total amount of polymeric aggregates formed in the system. Examples of the time evolution of Q obtained for the SPS (M_w = 36 × 10⁴)/$CDCl_3$ system at various concentrations C and temperatures T are shown in Figure 3a (the C dependence at 10 °C) and 3b (the T dependence for C = 7.57 g/dL). Here, the Q's are normalized to the values obtained for 1 mm cell thickness and 30 min integration by the PSD positioned at L = 4.0 m. In every case the Q increases monotonically with gelation time.

2. Conformational Ordering on Gelation. In ref 11, the conformational ordering process on gelation of the SPS/$CHCl_3$ system is monitored with the absorbance of the conformation-sensitive IR band at 572 cm^{-1}, which is associated with ordered sequences of the TTGG skeletal conformation. In IR spectra of SPS and IPS, there are observed many conformation-sensitive bands associated with the regular sequences of each particular skeletal conformation (TTGG and TT for SPS and TG for IPS) equal to or longer than certain limiting lengths (the critical sequence lengths) which are necessary for the appearance of the respective bands.[12,13] The critical sequence length (represented by the number of monomeric units m constructing the sequence) is related to the sensitivity of the band to the conformational order. For the TG sequences of IPS, the m values for various IR bands have been evaluated through the intramolecular isotope-dilution technique.[12−14] The m value of the 572 cm^{-1} band of SPS is assumed to be ca. 8 [that corresponds to two turns of the (2/1) helix consisting of eight monomeric residues linked in the ordered TTGG skeletal conformation] by analogy with the IPS band at 566 cm^{-1}.

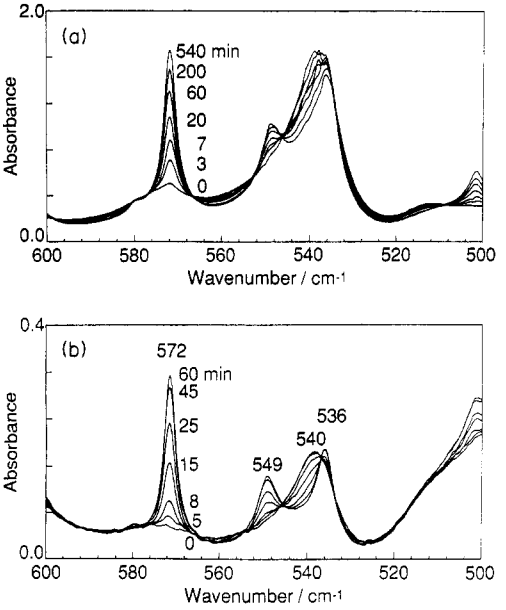

Figure 4. Time-resolved FT-IR spectra on gelation of SPS (M_w = 36 × 10⁴)/$CHCl_3$: (a) C = 8.05 g/dL measured at 10 °C; (b) C = 1.09 g/dL measured at −5 °C.

Some examples of the time dependency of the IR spectrum measured on SPS (M_w = 36 × 10⁴, C = 8.05 and 1.00 g/dL)/$CHCl_3$ solutions measured at 0 and −5 °C are reproduced in Figure 4a,b. The absorbance of the 572 cm^{-1} band increases very slowly with gelation time. Through the following procedure, the absorbance is converted to an absolute scale that represents the conformational order of SPS molecules dispersed in gel. The sharp bands at 572, 549, and 536 cm^{-1} are due to the ordered TTGG sequences and increase in intensity with gelation time. The broad absorption with the peak at 540 cm^{-1}, which superposes the 549 and 536 cm^{-1} bands, as well as the broad background beneath the 572 cm^{-1} band, is associated with the monomeric residues accommodated in the segments of random conformation. They decrease in intensity on gelation.

The observed absorbance profile is separated into several components using a curve-fitting program, as shown in Figure 5. The appearance of clear isosbestic points in the time-resolved spectra (Figure 4) indicates that we are able to regard the conformational ordering as a two-component reaction from the disordered (represented by the subscript B) to the ordered state (represented by A). In that case the integrated intensities of a selected band-pair of the ordered (I_A) and disordered monomeric residues (I_B) are expressed by the equations

$$I_A = \epsilon_A x_A c l \qquad (3)$$

$$I_B = \epsilon_B (1 - x_A) c l = \epsilon_B c l - (\epsilon_B/\epsilon_A) I_A \qquad (4)$$

where ϵ_A and ϵ_B denote the molar absorption coefficients,

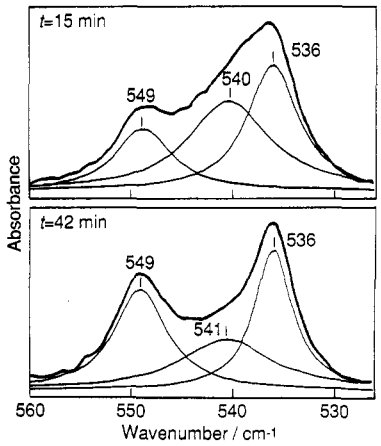

Figure 5. Examples of curve fitting of time-resolved FT-IR spectra measured for SPS (M_w = 36 × 10^4, C = 1.09 g/dL)/$CHCl_3$ gel after gelation times of 15 and 42 min at −5 °C.

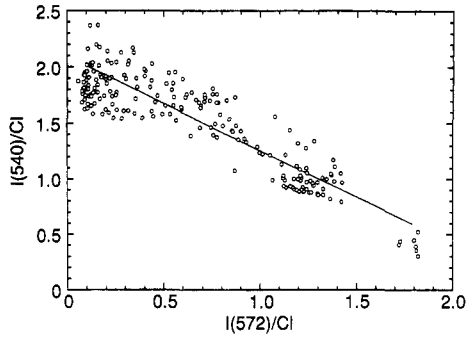

Figure 6. $I(540)/Cl$ versus $I(572)/Cl$ plot for SPS (M_w = 36 × 10^4)/$CHCl_3$ gels obtained at various concentrations, temperatures, and gelation times. The slope gives the ratio of molar absorption coefficients $\epsilon(540)/\epsilon(572)$ = 0.838.

x_A and x_B are the weight fractions of the monomeric residues, respectively, in the ordered and disordered conformational states, c is the total molar concentration of the monomeric residues contained, and l is the path length of the optical cell used. According to eq 4, the I_B/cl versus I_A/cl plot obtained at various C's, T's, and gelation times (t) gives a common straight line with the slope of $-(\epsilon_B/\epsilon_A)$. Using the value of the ratio ϵ_B/ϵ_A thus obtained, we are able to evaluate the weight fraction x_A of the monomeric residues which are accommodated in the ordered TTGG sequences equal to or longer than the critical sequence length of the selected A band according to the equation

$$1/x_A = 1 + (I_B/I_A)(\epsilon_A/\epsilon_B) \quad (5)$$

In the present work, we used the 572 and 540 cm^{-1} bands as the A and B bands, respectively. The I_B/cl vs I_A/cl plot is shown in Figure 6, giving the value of the molar absorption coefficient ratio ϵ_B/ϵ_A = 0.838.

According to eq 5 $x_A = x(572)$ values evaluated for various sets of C, T, and t were plotted against $I_A/Cl = I(572)/Cl$, giving a common straight line, as shown in Figure 7. Here, the polymer concentration C is expressed in g/dL. By using the slope of this line, the reduced integrated intensities of the 572 cm^{-1} band $I(572)/Cl$ are converted to an absolute scale of the conformational order for the SPS molecules $x(572)$, which denotes the weight fraction of the monomeric residues accommodated in the ordered TTGG sequences equal to or longer than two turns of the (2/1) helix [$x(572) = 2.50 \times I(572)/Cl$].

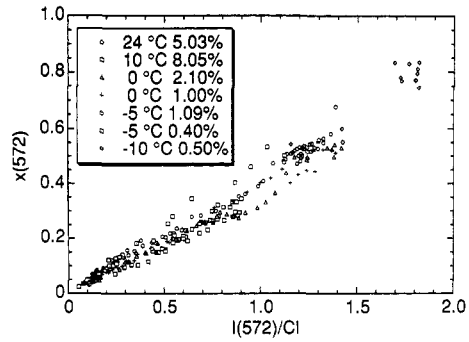

Figure 7. Relationship between the reduced absorbance of the 572 cm^{-1} band, $I(572)/Cl$ and the conformational order parameter $x(572)$.

The time dependencies of $x(572)$ obtained for the SPS/$CHCl_3$ system at various C's and T's are shown in Figure 8a–f. The data points obtained at −10 °C scatter to a great extent, because the FT-IR spectra were measured at very dilute concentrations (C = 0.5 g/dL or lower) in order to suppress the rate of the conformational change in a suitable level measurable by the present time-resolved experiment, so that the spectra obtained were rather noisy. The results of the conformational ordering are to be compared with those of the gel-network formation obtained by SANS. By comparing, for example, Figure 3a with Figure 8c (both are measured at 10 °C for almost the same concentrations), we conclude that the conformational ordering of SPS molecules proceeds in parallel with the growth of molecular aggregates. The kinetics of the conformational ordering has been investigated in ref 11 in connection with the mechanism of stabilization of the ordered conformations.

Here we are concerned with the final state of the gelation process. In a comparatively low temperature range (at 10 °C or lower), $x(572)$ tends to level off to a maximum value $x_m(572)$ that depends on temperature. This suggests that after a time long enough to construct gel networks the SPS/$CHCl_3$ system arrives at the equilibrium state. The $x_m(572)$ values evaluated at various temperatures are listed in Table 1. The result shows that in SPS gels formed at −10 °C, 70% of monomeric residues of SPS molecules are accommodated in the ordered TTGG sequences equal to or longer than two turns of the (2/1) helix even at a concentration as low as 0.2%.

If the statistical weights for the ordered (A) and disordered (B) conformational states of a monomeric residue at the equilibrium are assumed to be unity and σ, respectively, we are able to write σ as

$$\sigma = \exp(-\Delta G/RT) \quad (6)$$

and

$$\Delta G = G_B - G_A = \Delta H - T\Delta S \quad (7)$$

where ΔG, ΔH, and ΔS are Gibbs energy, enthalpy, and entropy differences per mole of monomeric unit, respectively, between the random and the helical states, R is the gas constant, and T is the absolute temperature.

For the simplest case where the state of a monomeric residue is not influenced by the states of the neighboring residues, the weight fraction $F(m)$ of the monomeric units which exists in the ordered sequences of length $\geq m$ is represented in terms of the probability p of finding a monomeric residue in the ordered conforma-

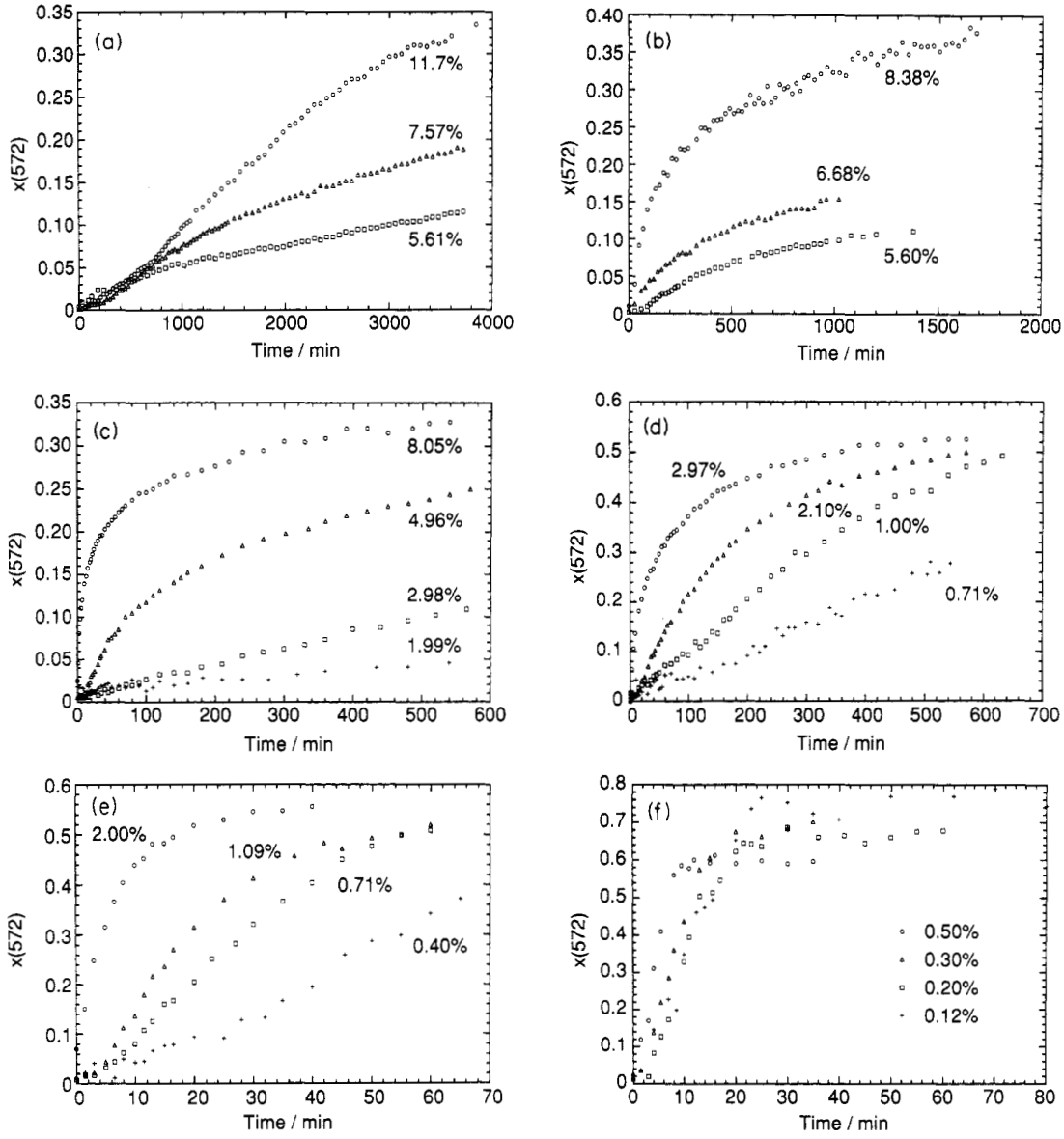

Figure 8. Time dependence of the conformational order parameter $x(572)$ on gelation of SPS ($M_w = 36 \times 10^4$)/$CHCl_3$ at various concentrations: (a) at 24 °C; (b) at 15 °C; (c) at 10 °C; (d) at 0 °C; (e) at −5 °C; (f) at −10 °C.

Table 1. Temperature Dependence of the Asymptotic Conformational Order of Syndiotactic Polystyrene Molecules in Gels Dispersed in Chloroform

	−15 °C	−10 °C	−5 °C	0 °C	10 °C
$x_{m(572)}$	0.76	0.70	0.57	0.53	0.33
p	0.88	0.86	0.82	0.81	0.74
L_n	8.6	7.3	5.6	5.3	3.8
L_w	16.2	13.5	10.1	9.5	6.6

tional state as

$$F(m) = p^{m-1}[m - (m-1)p] \tag{8}$$

and σ is given by

$$\sigma = (1-p)/p \tag{9}$$

Since $x_m(572) = F(8)$ in the present case, we are able to evaluate the values of σ as a function of temperature. The $-R \ln \sigma$ vs $1/T$ plot gives a straight line whose slope and intercept provide ΔH (=24 kJ/mol of monomeric unit) and ΔS (=77 J K^{-1}/mol of monomeric unit), respectively (Figure 9). The magnitudes of ΔH and ΔS

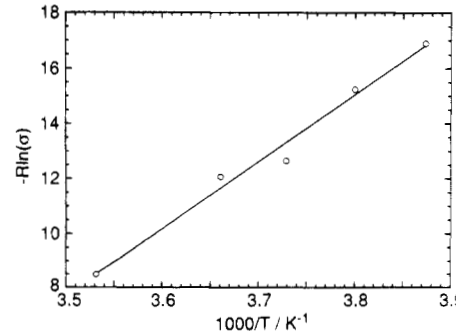

Figure 9. $-R \ln \sigma$ versus $1/T$ plot for SPS/$CHCl_3$ gels.

are about 2 times greater than the corresponding ones obtained for the IPS/CS_2 system.[12]

From the values of σ or p, the number average L_n and weight average lengths L_w of the ordered TTGG sequences (represented by the number of the monomeric residues) are obtained according to the equations

$$L_n = 1/(1-p) \tag{10}$$

and

$$L_w = (1 + p)/(1 - p) \quad (11)$$

The values of $F(8) = x_m(572)$, p, L_n, and L_w at various temperatures are summarized in Table 1.

The above consideration is based on the assumption that the gel state is the equilibrium state which the SPS/$CHCl_3$ system approaches. However, validity of this assumption is still uncertain. In fact, around room temperature occurrence of additional far slower structural changes are observed by SANS and FT-IR. For example, at 24 °C, the $x(572)$ changes in a complicated fashion; it tends to level off first and then increases again (see Figure 8a). Moreover, it was found that the SANS profile of an SPS/$CDCl_3$ sample stored at room temperature continued to change in the time scale of months accompanied by a substantial increase in cloudiness of the gel. These findings suggest that the gel state of the SPS/$CHCl_3$ system is possibly a metastable state realized on the pathway from the solution to the final state.

3. Structural Change of Molecular Aggregates on Gelation. In this subsection we deal with the change in aggregation state of polymer molecules revealed by quantitative analyses of the time-resolved SANS functions.

As described in a previous paper,[15] the $I(q)$ functions obtained for well-developed SPS-d_8/CCl_4 and SPS/o-$C_6D_4Cl_2$ gels were reproduced by the following theoretical equation derived by Freltoft et al. for continuous fractal objects[16]

$$I(q) = BP(q)\,S(q) \quad (12)$$

with

$$P(q) = \exp\left(-\frac{1}{5}q^2r_0^2\right) \quad (13)$$

and

$$S(q) = 1 + \frac{K\Gamma(D_m - 1)\xi^{D_m}\sin[(D_m - 1)\tan^{-1}(q\xi)]}{q\xi(1 + q^2\xi^2)^{(D_m-1)/2}} \quad (14)$$

Here, r_0 denotes the radius of unit particles constructing the polymeric clusters (the lower cutoff length), ξ is the correlation length (the upper cutoff length on which the clusters are nonuniform), B and K are proportionality constants, and $\Gamma(x)$ means the Gamma function of the variable x.

For the case of the SPS/$CDCl_3$ system, the $I(q)$ functions obtained for the gels after standing for a long time at a comparatively low temperature are also reproducible by eq 12 (combined with eqs 13 and 14) as shown in Figure 10 for the case of SPS ($M_w = 36 \times 10^4$, C = 7.57 g/dL)/$CDCl_3$, kept for 550 min at 15 °C (corresponding to the uppermost curve in Figure 2). The structural parameters evaluated by the least squares fitting are r_0 = 4.75 nm, ξ = 6.16 nm, and D_m = 2.43.

For the case of the $I(q)$ function of the same sample measured at 24 °C, the shape of the double logarithmic plot of $I(q)$ vs q changes rather gradually, as shown in Figure 11. The $I(q)$'s obtained at an early stage of gelation (t < 300 min) exhibit a characteristic shape different from those of both well-grown gels and linear polymer solutions. The shape is very close to that of semidilute solutions of star polymers reported by Dozier et al.[17] The SANS functions of this type cannot be reproduced by eq 12. Dozier et al. presented the following theoretical equation that reproduces well SANS functions of this type[17]

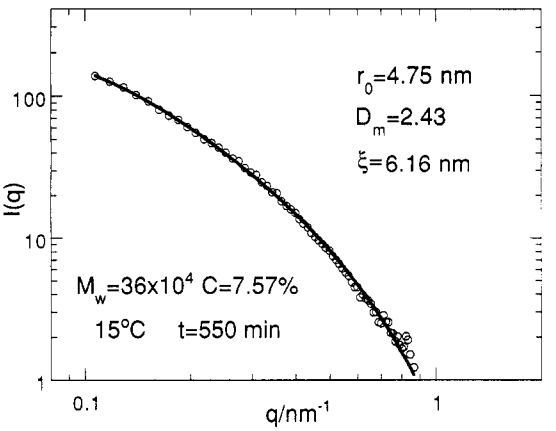

Figure 10. Least squares fitting of eq 12 (with eqs 13 and 14) to the measured SANS intensity $I(q)$ data obtained for SPS ($M_w = 36 \times 10^4$, C = 7.57 g/dL) sample after gelation time of 550 min at 15 °C. The values of the structural parameters are given.

$$I(q) = I(0)\exp\left(-\frac{1}{3}q^2R_g^2\right) + \frac{K'\Gamma(D' - 1)\sin[(D' - 1)\tan^{-1}(q\xi')]}{q\xi'(1 + q^2\xi'^2)^{(D'-1)/2}} \quad (15)$$

where R_g represents the radius of gyration of stars, ξ' and D' are the correlation length and the mass-fractal dimension, respectively, inside the star, and K' is a proportionality constant. The reciprocal of D' is the Flory exponent ν which varies from 0.5 (for a Gaussian chain) to 1.0 (for a rodlike chain).

This equation has not been derived from a star-shaped molecular model but has been constructed by joining two terms; the first term of the right-hand side of eq 15 represents the scattering in a small q range due to the ensemble of spherical coagulates dispersed in a medium, and the second term is due to the mass pair-correlation function inside the sphere which gives rise to the scattering covering a wide q range. When the contribution of the first term exceeds that of the second one, eq 15 reproduces well the SANS functions obtained at an early stage of gelation. In fact, the curve obtained at t = 11 min in Figure 11 is reproduced by this equation with the set of structural parameters R_g = 19.8 nm, ξ' = 3.58 nm, and D' = 1.13 (or ν = 0.89), as shown by the solid line. The SANS functions obtained within t = 300 min exhibit the same shape. It is noticeable that these SANS functions give rise to a linear portion in the Guinier plot [the ln $I(q)$ vs q^2 plot], and the R_g values evaluated from the slope are coincident with those obtained from eq 15.

Beyond t = 400 min the $I(q)$ tends to change the shape, as shown by the curve obtained at t = 470 min in Figure 11. This curve is also reproduced by eq 15 with R_g = 18.6 nm, ξ' = 11.5 nm, and D' = 1.36 (ν = 0.74). According to the physical meaning of the parameters in eq 15 ξ' should be far smaller than R_g. However, the SANS data obtained around t = 450 min give the ξ' comparable to or even greater than R_g in some cases. In this stage the linear portion of the Guinier plot is limited to a very small q range. The $I(q)$ functions of this type are obtained in a rather narrow range of gelation times.

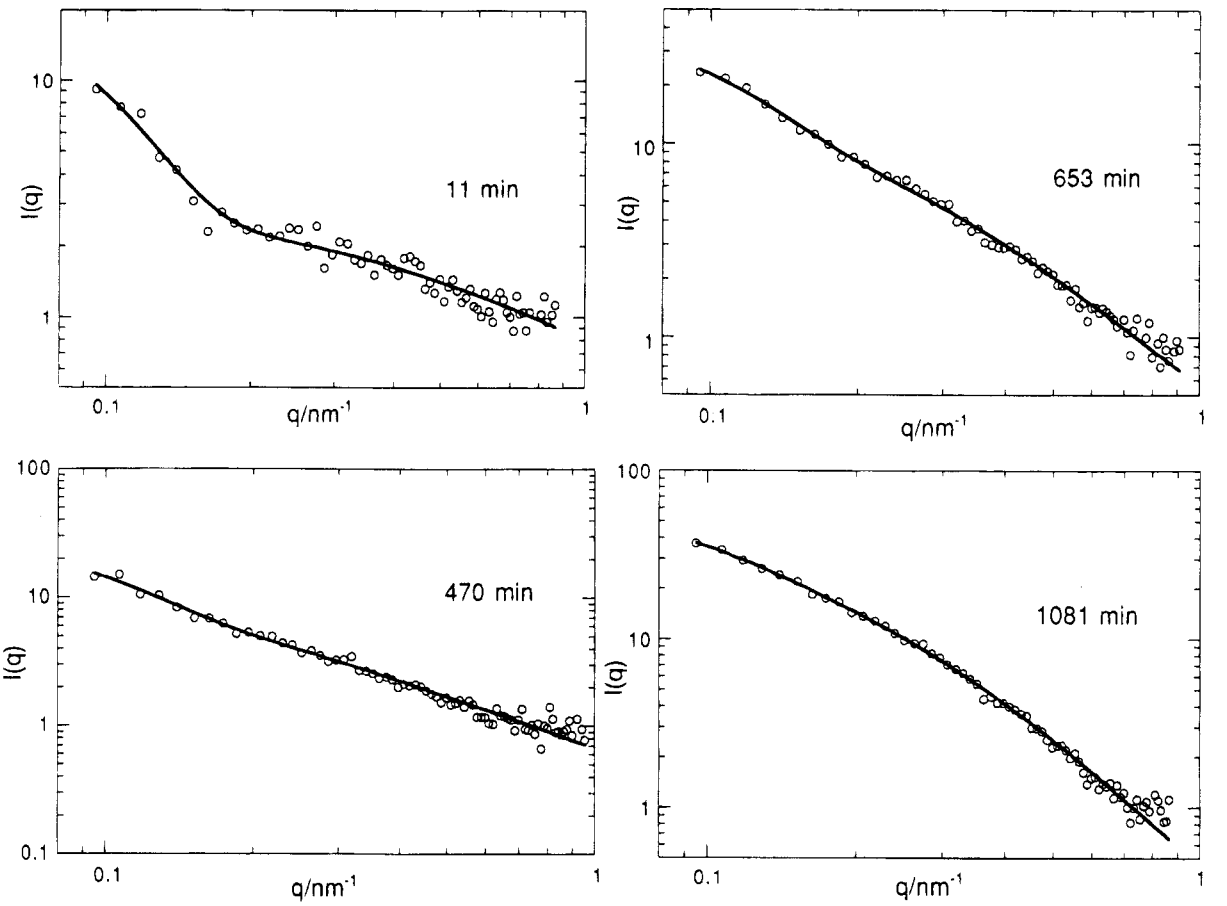

Figure 11. Time dependence of SANS function $I(q)$ measured for SPS ($M_w = 36 \times 10^4$, $C = 7.57$ g/dL)/$CDCl_3$ at 24 °C.

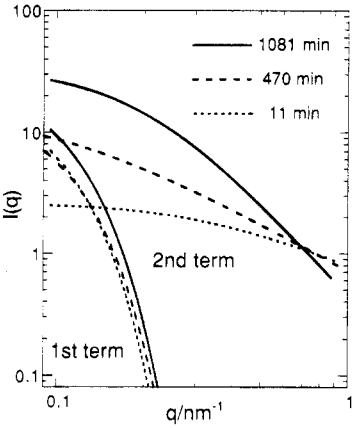

Figure 12. Time dependencies of the contributions from two terms in the right-hand side of eq 15 obtained for SPS ($M_w = 36 \times 10^4$, $C = 7.57$ g/dL)/$CDCl_3$ at 24 °C.

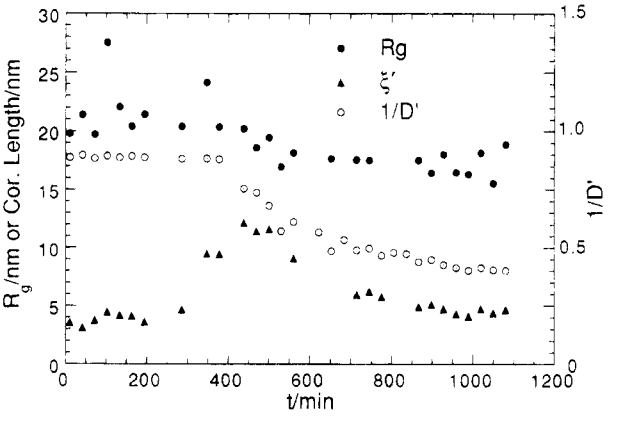

Figure 13. Time dependencies of structural parameters evaluated by a least-squares fitting of eq 15 to the time-resolved SANS data obtained for the SPS ($M_w = 36 \times 10^4$, $C = 7.57$ g/dL)/$CDCl_3$ sample at 24 °C.

As the gelation proceeds further ($t > 600$ min) the shape of $I(q)$ approaches that of well-grown gels obtained at a lower temperature (Figure 10). The SANS functions obtained in such a late stage are reproduced by eq 12 (for example, the data at $t = 1081$ min gives the parameters $r_0 = 2.85$ nm, $\xi = 11.5$ nm, and $D_m = 2.06$). The Guinier plot of the data obtained in that stage does not give rise to any linear portion until the lowest q range.

From the theoretical viewpoint eq 15 is valid only for the $I(q)$'s obtained in some early stage of gelation. Nevertheless, the data obtained throughout the whole gelation process are reproduced, at least apparently, by eq 15, as shown by the solid lines in Figure 11. This fact is due to the functional form of the second term in the right-hand side of eq 15. This term is essentially the same as the second term of the right-hand side of eq 14, except for the factor ξ^{D_m}. As the gelation proceeds, the contribution of the second term increases monotonically, whereas that of the first term remains almost constant (Figure 12). Therefore, as the gelation goes to a late stage, eq 15 approaches eq 12 and reproduces apparently the SANS functions obtained in that stage, although the parameters involved lose their own physical meanings. In this respect, eq 15 is available only for the $I(q)$'s obtained in the early stage.

Although there might be some difficulties in analyzing the SANS data obtained in the whole gelation process according to eq 15, we considered the time evolution of polymeric aggregates on the basis of the change in the

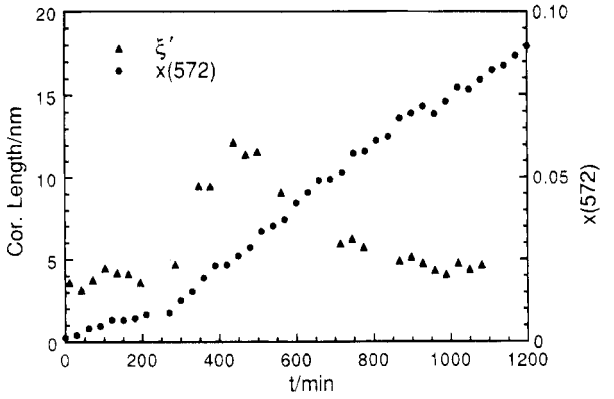

Figure 14. Comparison of time dependencies between the conformational order parameter $x(572)$ and the correlation length ξ', obtained for SPS ($M_w = 36 \times 10^4$, $C = 7.57$ g/dL)/ chloroform at 24 °C.

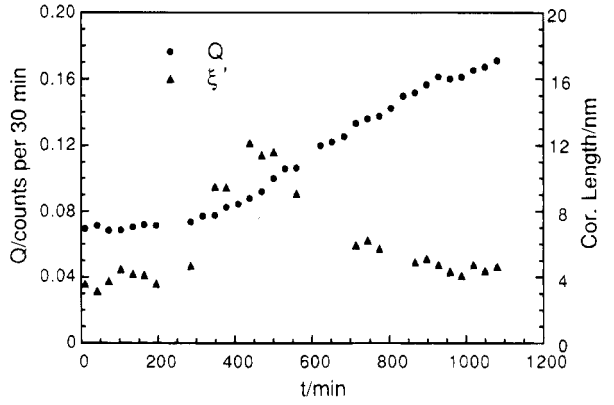

Figure 15. Comparison of time dependencies between the partial invariant Q and the correlation length ξ' obtained for SPS ($M_w = 36 \times 10^4$, $C = 7.57$ g/dL)/$CDCl_3$ at 24 °C.

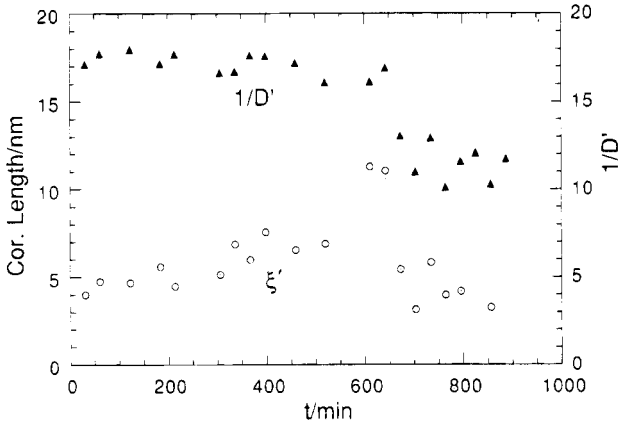

Figure 16. Time dependencies of the ξ' and ν ($=1/D'$) parameters (in eq 15) obtained for SPS ($M_w = 36 \times 10^4$, $C = 6.48$ g/dL)/$CDCl_3$ at 24 °C.

structural parameters derived by a nonlinear least-squares fitting of eq 15 to the SANS data. Figure 13 shows the time dependence of a set of the structural parameters R_g, ξ', and ν ($=1/D'$). The correlation length ξ' inside the star increases very slowly in the early stage of gelation, then rapidly increases in a divergence-like manner around $t = 450$ min. Thereafter, it decreases toward a constant value (ca. 5 nm). The Flory exponent ν assumes a large constant value of ca. 0.85 in the early stage, then decreases sharply accompanied with the sharp increase of ξ', and then approaches a constant value of ca. 0.5. Contrary to these two parameters, R_g remains almost constant throughout the whole gelation process.

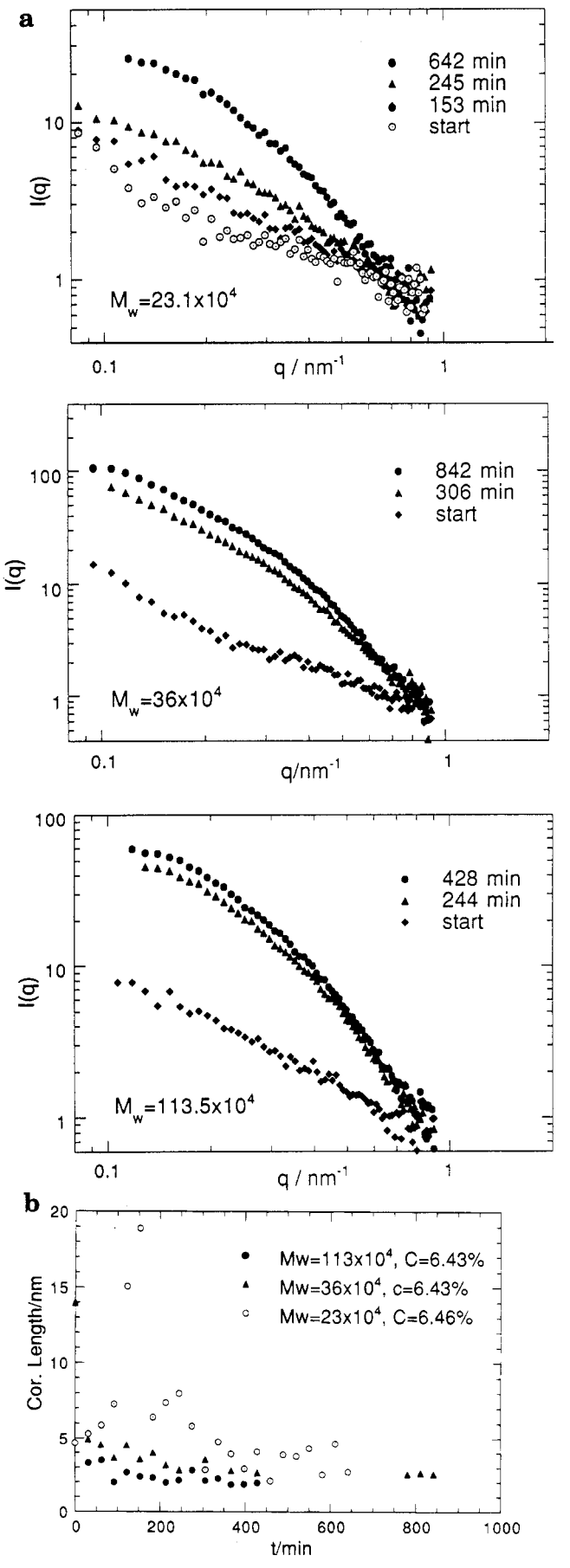

Figure 17. Effect of molecular weight of SPS on time dependencies of (a) the $I(q)$ function and (b) the correlation length ξ' obtained for SPS/$CDCl_3$ samples (C = ca. 6.45 g/dL) at 15 °C.

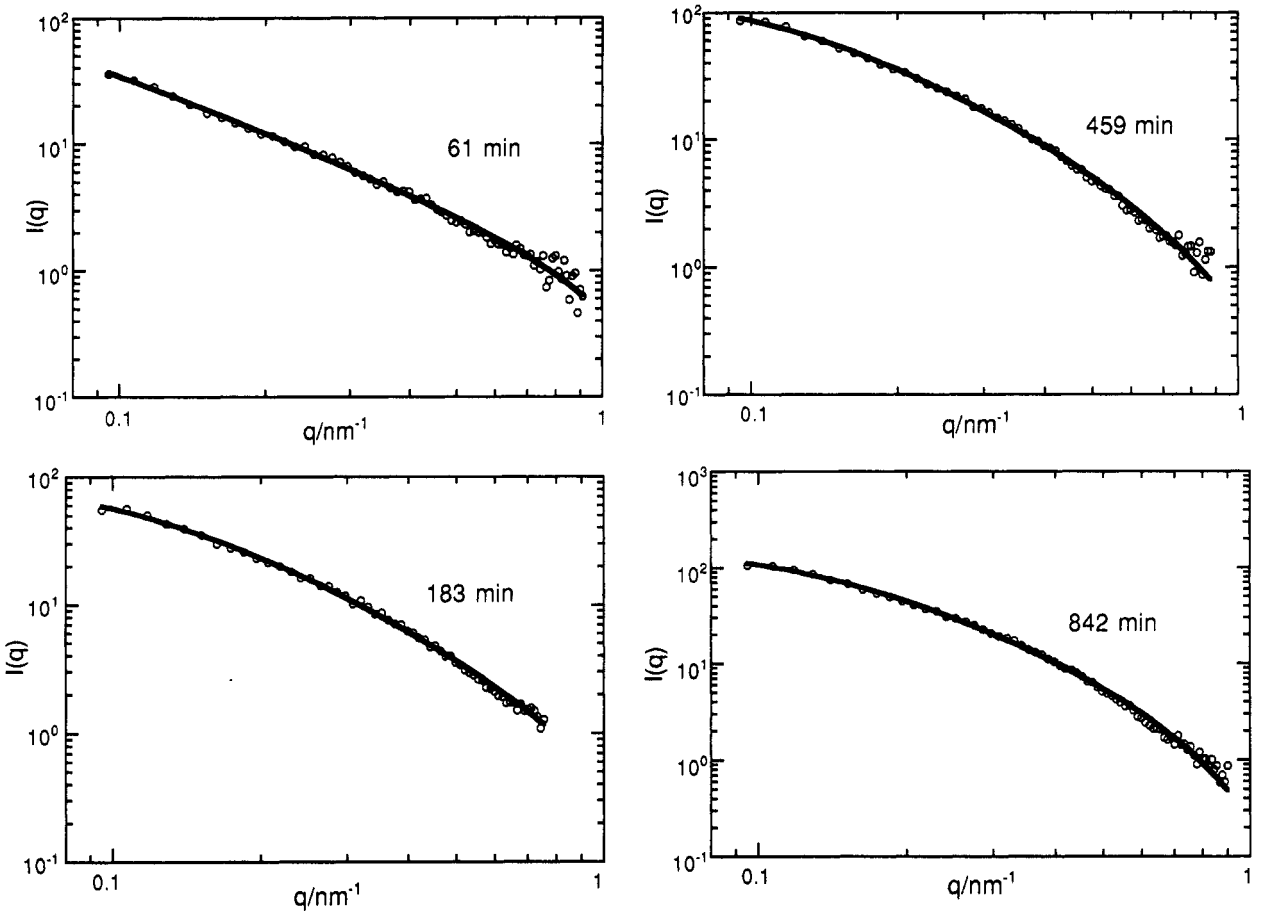

Figure 18. Time evolution of the SANS function measured for SPS ($M_w = 36 \times 10^4$, $C = 6.43$ g/dL)/$CDCl_3$ at 15 °C and the result of least-squares fitting using eq 12 (solid curves).

It is noticeable that the ξ' and ν parameters exhibit a very abrupt change at a particular narrow range of gelation times. The divergence-like sharp increase of ξ' is especially prominent. This change is presumably due to the change in the aggregation state from dispersed islands to a continuum, corresponding to the occurrence of a sol–gel transformation. In fact, the conformational order $x(572)$ (Figure 14) and the partial invariant Q, a measure of the amount of polymeric aggregates formed (Figure 15), start to increase at the same point. Divergence of the correlation length is commonly observed for various critical phenomena.

The characteristic features of time dependencies of these structural parameters are common in all cases of SPS/$CDCl_3$ gels examined, although the time scale of the variation depends on M_w, C, and T, as will be described in what follows. Figure 16 shows the time dependencies of ξ' and ν ($=1/D'$) for the case of $M_w = 36 \times 10^4$, $C = 6.48$ g/dL measured at 24 °C. In comparison with Figure 13, the result indicates that as C is lowered, the occurrence of the sol–gel transformation is shifted to a longer gelation time ($t = 600$ min). The effect of molecular weight M_w on variation of ξ' was investigated at 15 °C for the samples of nearly the same concentration (ca. 6.5 g/dL) as shown in Figure 17. For the cases of $M_w = 113 \times 10^4$ and 36×10^4, the divergence of ξ' was not detectable because the sol–gel transformation is completed within the first run of the time-resolved SANS measurement at this temperature, and the occurrence of the transformation was detected only for $M_w = 23 \times 10^4$ around $t = 200$ min.

The sol–gel transformation mentioned above takes place in an early stage of gelation and, therefore, is detectable only for some limited cases of low molecular weight, low concentration, and/or comparatively high temperature.

Because of the limitation in validity of eq 15, the changes of the structural parameters obtained in the gelation stage after the transformation regime are difficult to discuss in connection with the actual structural change of polymeric aggregates. For that stage the time dependencies of the structural parameters were obtained by the least squares fitting of eq 12. Figure 18 shows the time evolution of the $I(q)$ function for the case of $M_w = 36 \times 10^4$, $C = 6.43$ g/dL at 15 °C, where the transformation regime is included within the first run, and all the $I(q)$ functions obtained after that are reproduced well by eq 12, as shown by the fitting with the solid curves. The time dependencies of the structural parameters for that case, along with the case of $C = 7.57$ g/dL, are shown in Figure 19. As gelation proceeds, the unit particle size r_0 and mass-fractal dimension D_m tend to increase, while the correlation length ξ decreases. The same tendency is seen in every case we investigated.

We have discussed the irreversible structural changes of the SPS/$CHCl_3$ system from homogeneous solution to gel occurring in the time scale of tens of hours. Figures 3 and 8 show that the scattering intensity Q as a measure of the amount of molecular coagulates formed and the conformational order parameter $x(572)$ increase monotonously with time and tend to level off to a limiting value characteristic of the temperature at which the gelation proceeds. Around room temperature, these changes proceed very slowly even for concentrated samples. These experimental results tell us that SPS/

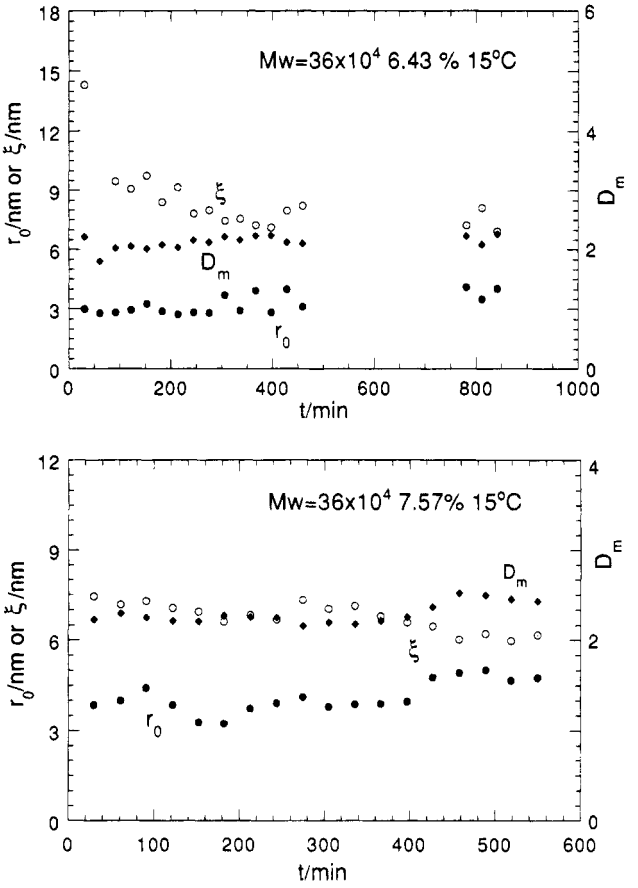

Figure 19. Time dependencies of structural parameters evaluated by a least-squares fitting of eq 12 to the time-resolved SANS functions obtained in the gelation stage after the transformation regime for SPS (M_w = 36 × 10^4)/$CDCl_3$ samples with C = 6.43 and 7.57 g/dL at 15 °C.

$CHCl_3$ solution cooled below a certain temperature is in a nonequilibrium state, and the molecular conformation as well as the aggregation state change toward an equilibrium structure. As for the final state to be attained, it is unclear at present whether the ordering process converges to the formation of a tightly bound continuum (gelation) or it converts to the deposition of crystalline particles segregated from the medium (crystallization). Presumably, there exists one or more metastable structures on the pathway to the final state. For the structural changes that occur in the SPS/solvent systems during longer time scales (several months), the results will be reported elsewhere.

References and Notes

(1) Immirzi, A.; de Candia, F.; Ianneli, P.; Zambelli, A. Vittoria, V. *Makromol. Chem., Rapid Commun.* **1988**, *9*, 761.
(2) Vittoria, V.; de Candia, F.; Ianneli, P.; Immirzi, A. *Makromol. Chem., Rapid Commun.* **1988**, *9*, 765.
(3) Kobayashi, M.; Nakaoki, T.; Ishihara, N. *Macromolecules* **1989**, *22*, 4377.
(4) Guerra, G.; Vitagliano, V. M.; De Rosa, C.; Petraccone, V.; Corradini, P. *Macromolecules* **1990**, *23*, 1539.
(5) Corradini, P.; Napolitano, R.; Pirozzi, B. *Eur. Polym. J.* **1990**, *26*, 157.
(6) Greis, O.; Xu, Y.; Asano, T.; Petermann, J. *Polymer* **1989**, *30*, 590.
(7) De Rosa, C.; Rapacciiuolo, M.; Guerra, G.; Petraccone, V.; Corradini, P. *Polymer* **1992**, *33*, 1423.
(8) Chatani, Y.; Shimane, Y.; Inoue, Y.; Inagaki, T.; Ishioka, T.; Ijitsu, T. Yukinari, T. *Polymer* **1992**, *33*, 488.
(9) Kobayashi, M.; Nakaoki, T.; Ishihara, N. *Macromolecules* **1990**, *23*, 78.
(10) Nakaoki, T.; Kobayashi, M. *J. Mol. Struct.* **1991**, *242*, 315.
(11) Kobayashi, M.; Kozasa, T. *Appl. Spectrosc.* **1993**, *47*, 1417.
(12) Kobayashi, M.; Tsumura, K.; Tadokoro, H. *J. Polym. Sci., Polym. Phys. Ed.* **1968**, *6*, 1493.
(13) Kobayashi, M.; Akita, K.; Tadokoro, H. *Makromol. Chem.* **1968**, *118*, 324.
(14) Nakaoki, T.; Kobayashi, M. *Rep. Prog. Polym. Phys. Jpn.* **1991**, *34*, 359.
(15) Kobayashi, M.; Yoshioka, T.; Kozasa, T.; Tashiro, K.; Suzuki, J.; Funahashi, S.; Izumi, Y. *Macromolecules* **1994**, *27*, 1349.
(16) Freltoft, T.; Kjems, J. K.; Sinha, S. K. *Phys. Rev. B* **1986**, *33*, 269.
(17) Dozier, W. D.; Huang, J. S.; Fetters, L. J. *Macromolecules* **1991**, *24*, 2810.

MA950162T